Mass Outflow in Active Galactic Nuclei: New Perspectives
ASP Conference Series, Vol. TBD, 2001
D.M. Crenshaw, S.B. Kraemer, and I.M. George

X-Ray Absorption Associated with High-Velocity UV Absorbers

Bassem M. Sabra & Fred Hamann

Dept. of Astronomy, University of Florida, Gainesville, FL 32611

Joseph C. Shields

Dept. of Physics & Astronomy, Ohio University, Athens, OH 45701

Ian George

LHEA, NASA/GSFC, GreenBelt, MD 20771

Buell Jannuzi

NOAO, 950 North Cherry Ave., Tuscon, AZ 85719

Abstract. We present *Chandra* observations of two radio-quiet QSOs, PG 2302+029 and PG 1254+047. PG2302+029 has an ultra high-velocity UV absorption system ($\sim -56,000$ km s^{-1}), while PG 1254+047 is a Broad Absorption Line (BAL) QSO with detached troughs. Both objects are X-ray weak, consistent with the known correlation between $\alpha_{\rm ox}$ and the strength of the UV absorption lines. The data suggest that there is evidence that both objects are intrinsically weak X-ray sources, in addition to being heavily X-ray absorbed. The X-ray absorption column densities are $N_{\rm H} > 10^{22}$ cm^{-2} for neutral gas and the intrinsic emission spectra have $\alpha_{ox} > 2$. The data are fit best by including ionized (rather than neutral) absorbers, with column densities $N_{\rm H}^{PG2302} > 2.98 \times 10^{22}$ cm^{-2} and $N_{\rm H}^{PG1254} > 17.3 \times 10^{22}$ cm^{-2}. The degrees of ionization are consistent with the UV lines, as are the total column densities if the strongest lines are saturated.

1. Introduction

Almost all quasi-stellar objects (QSOs) are X-ray sources. The reprocessing of X-rays by matter along the line of sight to the QSO imprints informative features on the resulting spectrum. We are examining the X-ray properties of QSOs with intrinsic UV absorption lines. In this proceeding we discuss *Chandra* observations of the QSOs PG 2302+029 and PG 1254+047. The BAL QSO PG 1254+047 displays detached broad absorption lines ($FWHM \sim 10,000$ km s^{-1} centered at -20,000 km s^{-1}) in the UV (Hamann 1998). PG 2302+029 is peculiar for its ultra-high velocity ($\sim -56,000$ km s^{-1}) UV absorption lines with $FWHM \approx 4,000$ km s^{-1} (Jannuzi et al. 1996). The intrinsic nature of the absorber in PG 2302+029 was confirmed recently by line variability (Jannuzi

et al. 2001). Both objects are characterized by being faint X-ray sources. Our aim is to determine the properties of the X-ray spectrum, search for any signs of absorption, and define the relationship between the UV/X-ray absorbers. If the X-ray and UV absorbers are the same, then the -56,000 km s^{-1} velocity shift of the UV absorption lines in PG 2302+029 **is potentially** resolvable with ACIS, given sharp features **and** adequate signal-to-noise ratio.

The absorption from this type of objects originates in an outflow of matter from the central engine of the QSO. Determining the relation between the gases producing the X-ray and UV absorption has profound implications on the physics of wind formation and acceleration (e.g. Mathur et al. 1995; Murray et al. 1995). Standard analysis, which uses the absorption line troughs to derive the optical depths and column densities, typically implies that the total column densities are about 2 orders of magnitude lower than the X-ray absorbing columns. However, the discrepancy could be alleviated if the UV lines are more optically thick than they appear, e.g. partial coverage fills the line troughs and thus hides larger column densities (Hamann et al. 1998).

2. Observations

PG 2302+029 and PG 1254+047 were observed by *Chandra* using the Advanced Imaging Spectrometer (ACIS) on 7 January 2000 and 29 May 2000, respectively. The most recent (2 November 2000 and 29 February 2001 for PG 2302+029 and PG 1254+047, respectively) re-processed data released by the CXC were used. No filtering for high background or bad aspect times was done since we found that the data were relatively free from such problems. Data extraction and calibration was performed using version 1.4 of CIAO. XSPEC was used for rebinning and spectral analysis. We created the response matrix and ancillary response files by relying on calibration data provided when the chip temperature during observations was -120°.

We extracted the source counts from circular regions with radii of $5''$. Background regions were annuli with radii of $10''$ to $20''$. We obtained a total of 391 ± 21 counts for PG 2302+029 and 47 ± 8 counts for PG 1254+047. Table 1 gives a list of pertinent information about the two objects. The specta were binned to have at least 30 counts/bin (10 counts/bin for PG 1254+047). The spectral analysis discussed in this contribution includes energy bins below 0.5 keV. It has come to our attention that these bins may suffer from calibration problems. See Sabra & Hamann (2001) and Sabra et al. (2001) for a treatment where energy bins only above 0.5 keV are included.

Table 1. PG 2302+029 and PG 1254+047

Object	Obs. Date	Exp. (ksec)	[1]$N_H^{Gal.}$ (cm^{-2})	[2]z_{em}	z_{abs}	B (mag)
PG 2302	2000-01-07	48	5×10^{20}	1.044	0.695	16.30
PG 1254	2000-05-29	36	2×10^{20}	1.024	0.870	16.15

[1] Lockmann & Savage (1994). [2] NED.

3. Data Analysis and Results

Our procedure for spectral fitting is the following. We start by fitting a power law continuum ($\phi_E \propto E^{-\Gamma}$) absorbed only by the appropriate Galactic column

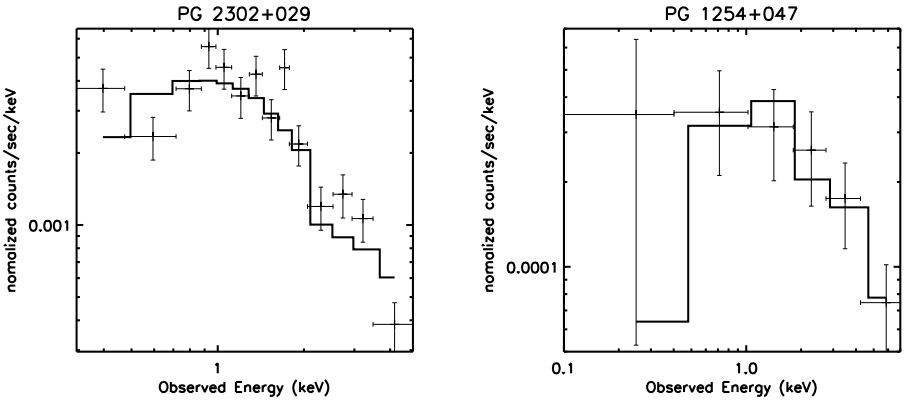

Figure 1. Galactic Absorption only, free normalization and Γ. PG 2303+029: $\phi_E = 6.88 \times 10^{-6}$ photon s^{-1} cm^{-2} keV^{-1} at 1 keV, $\Gamma = 1.071$, $\chi^2_\nu = 2.57$ for 12 d.o.f., PG 1254+047: $\phi_E = 6.63 \times 10^{-7}$ photon s^{-1} cm^{-2} keV^{-1} at 1 keV, $\Gamma = 0.3787$, $\chi^2_\nu = 0.45$ for 4 d.o.f.

density (Lockman & Savage 1994). Both the normalization of this continuum and its X-ray photon index, Γ, are left as free parameters. The results are shown in Figure 1. The slopes are rather flat for QSOs, where usually $1.3 < \Gamma < 2.3$ (e.g. Laor et a. 1997; Reeves et al. 1997). The X-ray fluxes are low, leading to the steep $\alpha_{\rm ox} = 2.1, 2.5$ for PG 2302+029 and PG 1254+047, respectively. These values are consistent with the correlation between $\alpha_{\rm ox}$ and the equivalent width of C IV $\lambda\lambda 1548, 1550$ shown in Figure 2, which was adapted from Brandt et al. (2000). The correlation is indicative of intrinsic absorption: a large equivalent width results from an absorber that, in turn, is accompanied by an X-ray absorber thus steepening α_{ox}.

To test for absorption, we adopt a "normal" QSO continuum, specified by $\alpha_{\rm ox} = 1.6$ and $\Gamma = 1.9$ (Laor et al. 1997), attenuated through a neutral absorber. The choice of α_{ox} determines the normalization of the powerlaw at 2 keV/(1+z), $\phi_E(1\ {\rm keV}) \propto f_\nu^{obs}(1\ {\rm keV})$, which we derive in the following way. We first calculate the rest-frame $f_\nu(2500\ {\rm \AA})$ from the B-magnitude, including the appropriate Galactic dereddening and the k-correction (see Green 1996). The rest-frame $f_\nu(2\ {\rm keV})$ and $f_\nu(2500\ {\rm \AA})$ are related by $\alpha_{ox} = 0.384\ log(f_\nu(2500\ {\rm \AA})/f_\nu(2\ {\rm keV}))$. Therefore, $f_\nu^{obs}(1\ {\rm keV}) \approx f_\nu^{rest}(2\ {\rm keV})/2)$, for $z \approx 1$. We experimented by adding neutral absorbers at the redshift of the QSO and at the redshift of the UV absorption lines. For PG 2302+029, the fits did not favour any particular redshift. The redshifts of the absorber and the QSO are too close to be resolved in PG 1254+047. In both cases, however, the X-ray absorption at the systemic velocity of the QSO leads to higher column densities (by a factor of less than 2). We hereafter fix the redshifts of the X-ray absorbers at those of the emission lines of the QSOs. The results are shown in Figure 3 below. The normalizations, based on higher energy channels where absorption has little effect, hint at intrinsic X-ray weakness, while the poor fits, especially at lower energies, hint at intrinsic absorption. The bad overall fit indicates that the observed X-ray weakness cannot be explained by absorption alone.

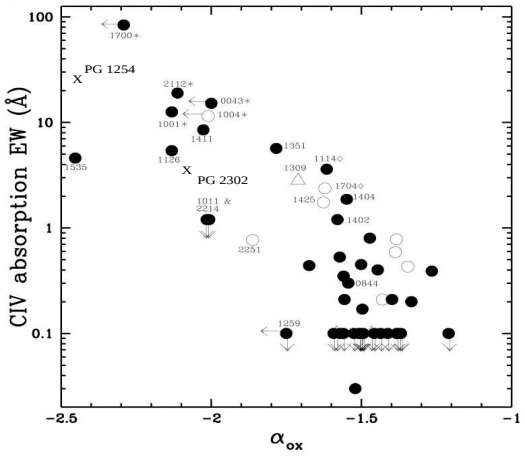

Figure 2. EW C IV vs. α_{ox}. Solid dots: radio-quiet QSOs, open triangles: core-dominated radio-loud QSOs, open circles: lobe-dominated radio-loud QSOs. Soft X-ray Weak QSOs are labeled their RAs, while an asterisk indicates a BAL QSO and a diamond signifies a warm absorber. We overplot our quantities for PG 2302+029 and PG 1254+047 as X's. We have recalculated our α_{ox} to be in agreement with the convention in this plot, i.e. between 3000 Å and 2 keV, instead of what we have used so (2500 Å and 2 keV) (Adapted from Brandt et al. 2000).

To study the possibility of both intrinsic X-ray weakness and absorption, we remove the constraint that $\alpha_{\rm ox} = 1.6$ and hence allow the normalization of the power law to vary. The fits improve drastically, though not to the extent of giving an acceptable fit ($\chi^2_\nu \approx 1$). The intrinsic power law flux density at 1 keV with these improved fits decreased by about an order of magnitude. We show the results in Figure 4.

The results from the above spectral fitting do not strongly support neutral absorption due to the large discrepancy between the data and the models at soft energies. Also, we know that there is not a neutral absorber with the above quoted column densities because the UV spectra do not contain low-ionization metal lines. To improve the fits, we experimented with absorption by ionized gas, and neutral and ionized partial coverage. We fix the ionization parameter U, the ratio of ionizing (above 13.6 eV) flux density to hydrogen density. Experiments showed that $logU = 0.1$ is consistent with UV data (Hamann 1998) and leads to $\chi^2_\nu < 2$. The partial covering fraction, $f_{\rm c}$, was fixed at 0.8 for PG 1254+047 because we found that it improved the quality of the fits. These values are consistent with absorption studies for such objects (e.g., Hamann 1998). Figure 5 displays the outcome.

The models in Figure 5 allow us to place limits on the column densities of the absorbers. We find that for PG 2302+029, $2.39 < \frac{N_H}{10^{22}\ cm^{-2}} < 3.66$, while for PG 1254+047, $6.73 < \frac{N_H}{10^{22}\ cm^{-2}} < 41.6$, both at the 90% confidence level.

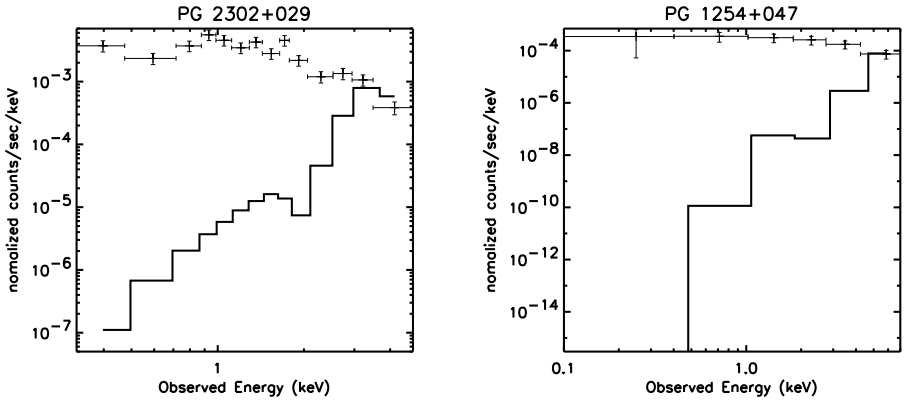

Figure 3. Galactic Absorption + Neutral Intrinsic Absorber, frozen normalization. PG 2302+029: $N_{\rm H} = 149.0 \times 10^{22}$ cm^{-2}, $\chi^2_\nu = 23.98$ for 13 d.o.f., PG 1254+047: $N_{\rm H} = 501.1 \times 10^{22}$cm^{-2}, $\chi^2_\nu = 6.28$ for 5 d.o.f.

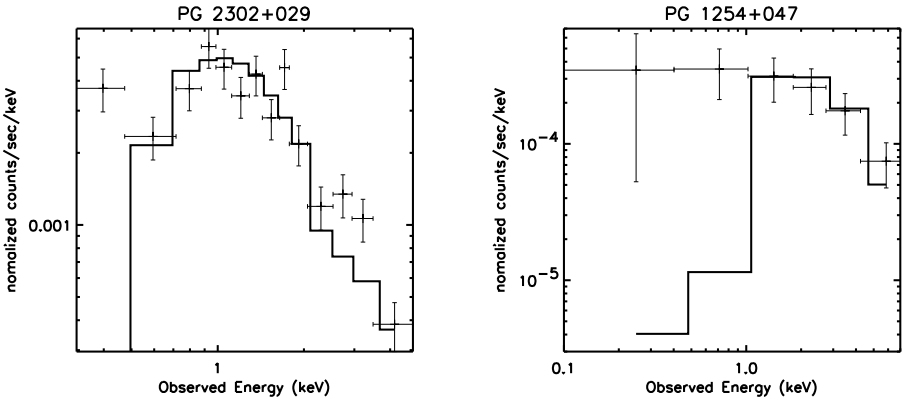

Figure 4. Galactic Absorption + Neutral Absorber, free normalization. PG 2302+029: $N_H = 1.12 \times 10^{22}$ cm^{-2}, $\phi_E = 1.36 \times 10^{-5}$ photon s^{-1} cm^{-2} keV^{-1} at 1 keV, $\chi^2_\nu = 3.57$ for 12 d.o.f., PG 1254+047: $N_H = 10.8 \times 10^{22}$ cm^{-2}, $\phi_E = 5.87 \times 10^{-5}$ photon s^{-1} cm^{-2} keV^{-1} at 1 keV, $\chi^2_\nu = 2.05$ for 4 d.o.f.

4. Conclusions

We have presented *Chandra* observations of PG 2302+029, a QSO that shows ultra high-velocity UV absorption, and PG 1254+029, a BAL QSO. The following points can be made:

1- The data suggest that there is evidence the both objects are intrinsically X-ray weak, though the X-ray slope is normal. The evidence is somewhat stronger for PG 2302+029 given the higher number of counts. No amount of absorbing column density was able to suppress the X-ray flux down to the observed values while at the same time reproduce the overall X-ray spectral shape. The intrinsic $\alpha_{\rm ox}$'s are steep: $\alpha_{\rm ox}^{\rm PG\ 2302} = 2.0$, $\alpha_{\rm ox}^{\rm PG\ 1254} = 2.3$.

2- There is intrinsic X-ray absorption, most probably ionized with $logU = 0.1$ and $N_{\rm H}^{\rm PG\ 2302} \gtrsim 2.98 \times 10^{22}$ cm^{-2}, $N_{\rm H}^{\rm PG\ 1254} \gtrsim 17.3 \times 10^{22}$ cm^{-2} for 80% partial

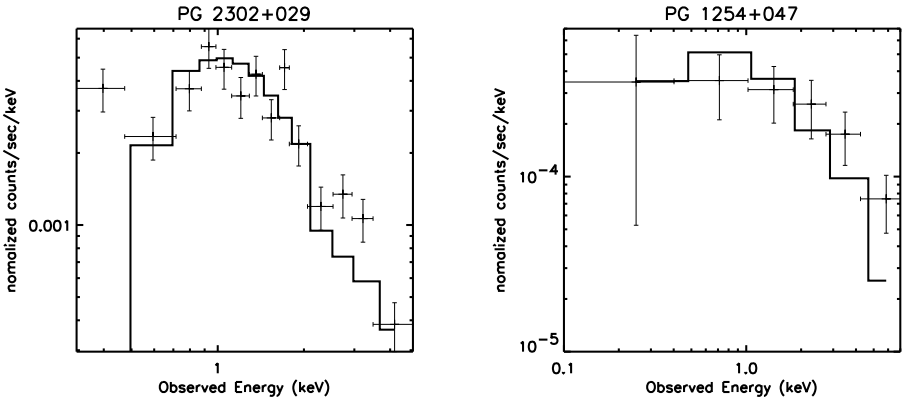

Figure 5. Galactic Absorption + Ionized Absorber, free normalization, partial coverage (PG 1254+047). PG 2302+029: $N_{\rm H} = 2.98\times10^{22}$ cm^{-2}, $logU = 0.1$ (frozen), $\phi_E = 1.54 \times 10^{-5}$ photon s^{-1} cm^{-2} keV^{-1} at 1 keV, $\chi^2_\nu = 1.66$ for 12 d.o.f., PG 1254+047: $N_{\rm H} = 17.3\times10^{22}$cm^{-2}, $logU = 0.1$ (frozen), $f_{\rm c} = 0.8$ (frozen), $\phi_E = 3.05 \times 10^{-6}$ photon s^{-1} cm^{-2} keV^{-1} at 1 keV, $\chi^2_\nu = 1.76$ for 4 d.of. The normalizations ϕ_E correspond to intrinsic $alpha_{\rm ox}$=2.0, 2.3, for PG 2302+029 and PG 1254+047, respectively.

coverage. The derived column densities are consistent with results from the UV data, if the UV lines are very saturated.
3- We were not able to determine the redshift of the X-ray absorber in PG 2302+029.

Acknowledgments. FH and BMS wish to acknowledge support through *Chandra* grants GO 0-1123X and GO 0-1157X.

References

Brandt, W. N., Laor, A., & Wills, B. J. 2000, ApJ, 528, 637
Hamann, F. 1998, ApJ, 500, 798
Jannuzi, B. T., et al. 1996, ApJ, 470, L11
Jannuzi, B. T., et al. 2001, in preparation
Laor, A., et al. 1997, ApJ, 477, 93
Mathur, S., Elvis, M., & Singh, K. 1995, ApJ, 455, L9
Murray, N., Chiang, J., Grossman, J. A., & Voit, G. M. 1995, ApJ, 451, 498
Sabra, B. M., & Hamann, F. 2001, ApJ Letters, to be submitted
Sabra, B. M., et al. 2001, ApJ Letters, to be submitted
Reeves, J. N., et al. 1997, MNRAS, 292, 468